Manipulation of light transmission through sub-wavelength hole array

2007 J. Opt. A: Pure Appl. Opt. 9 S450

(http://iopscience.iop.org/1464-4258/9/9/S28)

IOP Publishing JOURNAL OF OPTICS A: PURE AND APPLIED OPTICS

J. Opt. A: Pure Appl. Opt. **9** (2007) S450–S457 doi:10.1088/1464-4258/9/9/S28

Manipulation of light transmission through sub-wavelength hole array

J F Song[1] and R Proietti Zaccaria[2,3]

[1] State Key Laboratory on Integrated Opto-electronics, College of Electronic Science and Engineering, Jilin University, Changchun, 130023, People's Republic of China
[2] LaSIE, Department of Applied Physics, Osaka University, 2-1 Yamada-Oka, Suita, Osaka 565-0871, Japan
[3] BIONEM Laboratory, Magna Graecia University, Campus Germaneto, Viale Europa, 88100 Catanzaro, Italy

E-mail: sjf@email.jlu.edu.cn and remo@ap.eng.osaka-u.ac.jp

Received 5 February 2007, accepted for publication 27 July 2007
Published 24 August 2007
Online at stacks.iop.org/JOptA/9/S450

Abstract
The manipulation of light transmission through a sub-wavelength array of holes is described here. We show that, similarly to metallic gratings, periodicity realizes transmission enhancement also in dielectric gratings. Moreover, a comparison between single-hole and multi-hole slabs shows a strong connection between transmission enhancement and lattice periodicity. In the end, by considering a photonic crystal slab formed by anisotropic materials such as liquid crystals, fine tuning of transmission versus the wavelength can be achieved.

Keywords: sub-wavelength holes, Fano resonance, Wood anomaly, photonic crystal

M This article features online multimedia enhancements

(Some figures in this article are in colour only in the electronic version)

1. Introduction

In the last decade the transmission of light through an array of periodic sub-wavelength holes has attracted increasing attention because of its peculiar effects. Metallic slabs drilled with sub-wavelength holes have been investigated since the work of Ebessen and collaborators, where they showed that unexpected transmission peaks can be obtained for some resonant wavelengths [1]. Because of the metallic composition of the slab, the role of surface plasmon polaritons was analyzed in depth,and the authors reached the conclusion that plasmons play a fundamental role in the enhancement phenomenon [2–4]. However, further studies seem to show how plasmons could be useful, but not essential, to enhance transmission [5–12] or even to be a negative ingredient for such a phenomenon [13, 14]. In the present work we will focus our attention on a two-dimensional sub-wavelength dielectric slab, i.e. no metal is present anywhere in/on the structure. As an obvious consequence, we will not investigate further the direct contribution of surface plasmon polaritons to the transmission enhancement, but we will put the accent on the possibility of shifting the transmission and reflection peaks by acting either on the geometry of the slab or on an external electric field. Besides, a comparison between single-hole and multi-hole geometries will show how the periodicity is responsible for the transmission enhancement.

Because we chose to emphasize the sub-wavelength peculiarity, we can define two-dimensional sub-wavelength dielectric slabs as a sub-class of photonic crystal slabs where the holes (either areas with lower refractive index) have a diameter that is much smaller than the wavelength of the light. For such a reason, many of the characteristics and behaviors shown by such devices resemble the well-known two-dimensional photonic crystals. The main difference is that, while photonic crystals have infinite translational periodicity in any direction of the domain of definition, photonic crystal slabs are three-dimensional structures showing periodicity only in two directions. The solutions or modes of these devices belong to two different categories: *guided modes* and *quasi-guided modes*. The former are defined only inside the slab

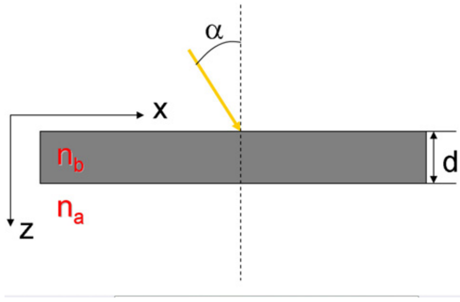

Figure 1. Uniform slab of thickness d and refractive index n_b surrounded by material of refractive index n_a. The light impinges on it from one side at an angle α. Both transmission and reflection are usually expected.

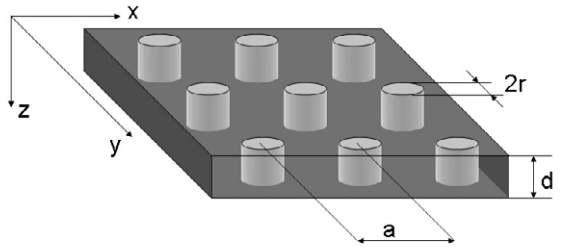

Figure 2. Photonic crystal slab formed by a square distribution of circular SiO_2 (light color) holes inside a layer of c-Si (dark color). Here we assume that $d = 0.5a$ is the slab thickness and $r = 0.15a$ is the hole radius, where a is the lattice period.

along its own symmetry plane and cannot couple with external radiation; the latter vice versa can couple with external light even though their energy is mainly confined inside the slab. Another definition of quasi-guided modes is Fano resonances, because they realize a coupling between a continuum and a discrete number of states [15]. Moreover, the usual definition of transverse electric (TE) and transverse magnetic (TM) polarizations valid for one- and two-dimensional photonic crystals must be slightly reconsidered. Indeed, for a photonic crystal slab, it is better to talk about *even* and *odd* modes: the former analogous to TE and the latter to TM [16]. The justification is that, while photonic crystals show an infinite and innumerable amount of mirror symmetry planes, a slab can show one of them only.

In [17], the authors introduced an alternative mathematical approach to solve the electromagnetic field distribution in anisotropic dielectric slabs numerically by using an extension of the scattering matrix method. Here we are going to apply such a method to show the geometry dependence of transmission peaks in two kind of structures: an isotropic crystal slab made out of c-Si and SiO_2 and a dielectric slab realized with liquid crystals embedded in between layers of SiO_2 material. In the last case an external electric field has the role of tuning the transmission peaks. The same method will also be used to investigate the influence of the periodicity on the transmission in isotropic crystal.

The paper is organized as follows. First, we introduce an example to show how geometrical and optical properties are linked to each other in photonic crystal slabs. For such a purpose, an isotropic slab realized by means of a background of c-Si periodically filled with SiO_2 is simulated. In particular, we explain how different behaviors can result according to which diffracted mode is observed. Next, to analyze the role played by the periodicity in the transmission, we compare a single-hole structure with a multi-hole structure. Finally, an anisotropic photonic crystal slab made out of liquid crystal is considered and the tuning of transmission by means of an external constant electric field is shown.

2. Isotropic structure

To review some of the optical properties of a photonic crystal slab, it is useful to start with the simple example of a non-absorbing uniform slab of thickness d and refractive index n_b in a background of refractive index n_a, as shown in figure 1. If light impinges on it from one side at an angle α to the normal to the interface, by means of the conservation relations of the components of electric and magnetic fields parallel and orthogonal to the interface, it is possible to calculate analytically both transmission and reflection. In the special case where the incident light is orthogonal to the surface ($\alpha = 0$), the relation defining reflection is:

$$r \propto (n_a - n_b)^2 \sin(k_b d) \quad (1)$$

where k_b is the wavevector in the slab. From equation (1), the condition for having zero reflection is simply $k_b = m\pi/d$, where m is an integer number (besides the trivial solution $n_a = n_b$, namely no refractive index modulation). Such a result is exactly the same that is obtainable by solving a quantum well or a Fabry–Perot etalon. If the incident light shows a non-zero angle α, a more general equation than (1) can be obtained [18], where reflection is proportional to $\sin(k_{b,z} d)$, where $k_{b,z}$ is the component of the $\mathbf{k}$ vector along the z direction inside the slab. However, no extra information is carried, namely the conditions for zero reflection are unchanged. By looking in detail at the resonant conditions, it is obvious that the transmission resonant peaks shift to higher wavelengths when the thickness of the slab increases or, in other words, both the angle α and the slab thickness d must be increased/decreased to maintain a resonant situation.

In the case where a periodic modulation of the refractive index is introduced into the slab, a structure such as in figure 2 is obtained. Along the directions x and y, holes with square periodicity are introduced, whereas along the z direction the structure is uniform. In particular, the holes are filled with SiO_2, and the slab is made out of crystalline silicon (c-Si) and is sandwiched between infinite layers of SiO_2. The refractive index is considered to be frequency independent, with values of 3.5 for c-Si and 1.46 for SiO_2. The radius r is $0.15a$ and the slab thickness d is $0.5a$, where a is the lattice constant.

It is well known [15] that coupling between a continuum with discrete states realizes asymmetric modes, which are also known as Fano's modes or Wood's anomaly [19]. Beside this, the mode asymmetry depends on many factors, such as the background [18] and the amount of available discrete levels. Figure 3 shows the total (all diffracted orders) transmission spectrum and the in-plane energy distribution on the top layer of the slab when the light is vertically incident with a wavelength of $\lambda = 2.066a$. Three Fano's peaks are present

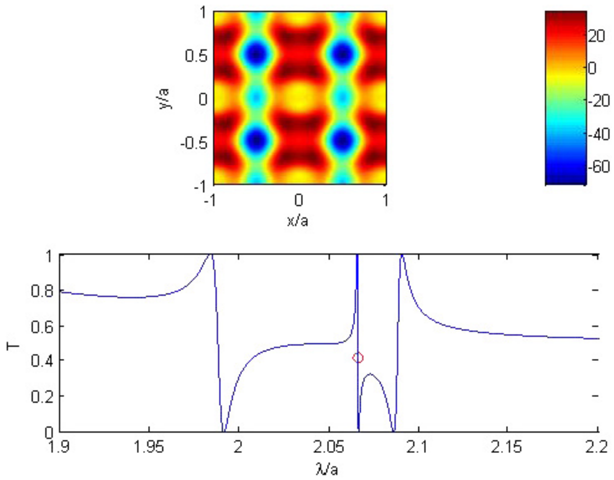

Figure 3. (Multimedia file of 2.6 Mb in AVI format available at stacks.iop.org/JOptA/9/S450) *c*-Si–SiO_2 photonic crystal slab with SiO_2 hole at (0, 0). The radius is $0.15a$ and the slab thickness is $0.5a$. The light is orthogonal to the top interface. Because of this, odd and even modes are degenerative (the structure manifests in-plane rotational symmetry). The bottom figure shows the total transmission spectrum versus wavelength. The (red) circle corresponds to $\lambda = 2.066a$. At the top, the associated in-plane energy distribution at $z = 0$ is illustrated. Positive values in the scale bar mean a Poynting vector parallel to the positive z axis (energy current entering the slab).

in the range of wavelengths from $1.9a$ to $2.2a$: at $1.987a$, $2.066a$ and $2.084a$. It is worthwhile looking at the scale which emphasizes the sharp energy distribution. In particular, the additional data related to figure 3 show that at the three Fano's peaks the energy is strongly confined in the slab, meaning a high in-plane Q factor. An alternative way to demonstrate such a statement is to look at the ratio $w/\delta w$, where w is the center of the resonance and δw is the line-width, which also defines the quality factor Q. Rough estimations for Q for the three resonant peaks are 330, 1400 and 370, respectively. The explanation is the occurrence of coupling between the incoming light and the quasi-guided modes of the slab. Vice versa, for non-resonant wavelengths, the light is not strongly confined in the slab, meaning direct transmission through the slab. This description is in agreement with the results obtained in [18], where two pathways in the transmission process were identified. Besides, Fano [15] had already presented an approach to describe the coupling between discrete and continuum states. It is worthwhile mentioning that in his case too, even though it could not look as straightforward as in [18], the two contributions, resonant and direct, were considered in a kind of quantum interference frame.

Because of the grating properties of the slab, when the device is illuminated from the top at an angle θ to the vertical (z direction), different scattered orders, both in reflection and transmission, can be expected (see figure 4(a)). Moreover, when the thickness of the slab changes, a shift of the relative intensity of the diffracted orders is observed. Such a behavior is analogous to the case of uniform slab discussed previously. However, because different diffracted orders are now expected, some substantial differences occur. In figure 4(b), the zeroth and first diffracted orders in transmission are shown. At $d = 0.497a$, $r = 0.15a$, $\theta = 20.47°$ and $\lambda = 1.5a$, the transmission ratio between the first- and the zeroth-order diffracted light is about 7000 (see figure 4(c)). From the results emerges clearly a high sensitivity toward the thickness variation. In particular, the resonant maximum for S_0 shifts to higher angles θ when the thickness is increased, whereas S_1 shows opposite behavior. This can be explained by using both

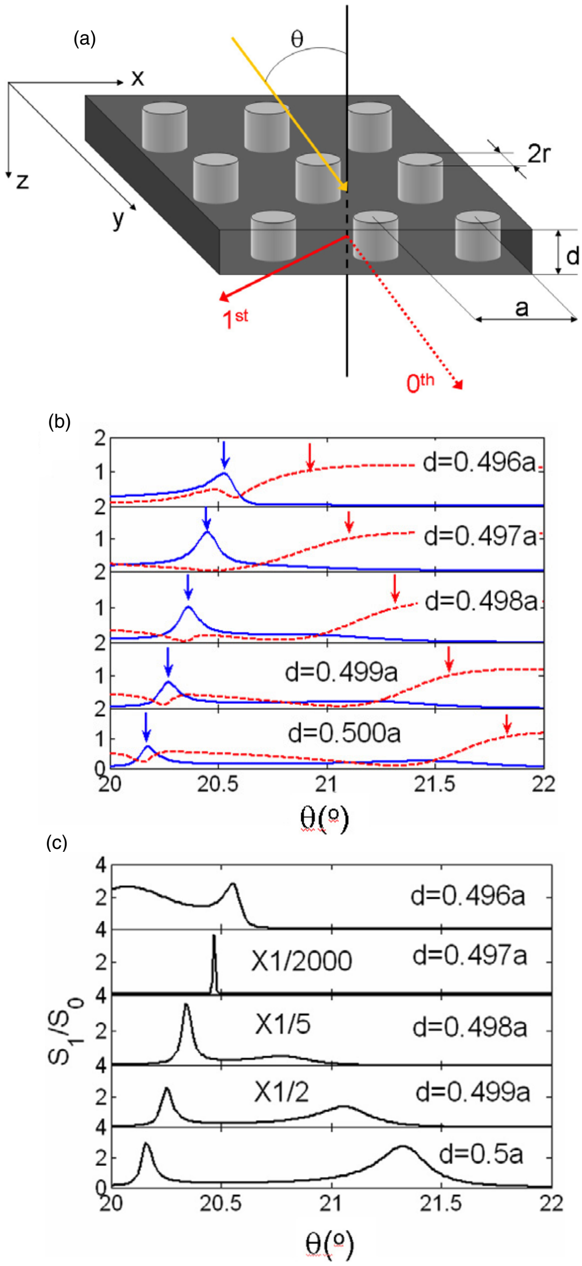

Figure 4. (a) Schematic representation of the zeroth and first scattered orders. The incoming light forms an angle θ with the vertical. The electric field is parallel to the y direction. (b) Transmitted light for the first two diffracted orders versus the angle θ. Each graph shows a situation with different slab thickness. The red arrows (dotted line) highlight the shift to higher angles of S_0 when the slab thickness increases. Vice versa, the blue arrows show the behavior of the first diffracted order (continuous line). (c) Ratio between the first-order and the zeroth-order diffracted light. At $d = 0.497a$ and $\theta = 20.47°$, the transmission ratio is about 7000. Here $\lambda = \lambda_0/n_{SiO_2} = 1.5a/1.46$ and $r = 0.15a$.

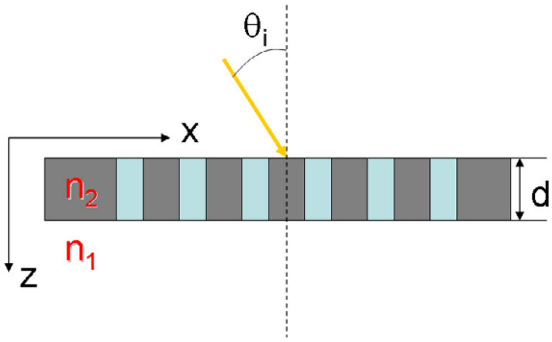

Figure 5. A system composed of a uniform medium of refractive index n_1 in contact with a photonic crystal slab of thickness d and effective refractive index n_2. Light of wavelength λ impinges on the slab at an angle θ_i to the normal at the interface.

the frame of the second Wood anomaly [19] and diffraction considerations all together. The phenomenon then consists in coupling between the diffracted orders and the eigenmodes of the slab and/or direct transmission through it. Because here we are not considering metallic structures, no surface plasmons can be excited. The remaining possibility is that the diffracted orders couple with quasi-guided modes of the device. In fact, as mentioned in the introduction, they are the only slab modes which can couple with external radiation. Hence, their mathematical expression is proportional to $e^{ik_z z}\Psi_{\mathrm{Bloch}}$, where the first factor takes into account the propagating component along the z direction, and Ψ_{Bloch} represents the Bloch modes traveling along the plane of the slab. The transmission resonance is dependent on the quantity $e^{ik_z z}$ which reveals the resonance conditions to have zero reflection. To understand in detail the results of figure 4, let us consider the sketch of figure 5. This represents a crystal slab of effective refractive index n_2 surrounded by a uniform material of refractive index n_1. Next, we will refer to variables related to the media with indexes 1 and 2, respectively. Light of wavelength $\lambda = \lambda_0/n_1$ (where λ_0 is the incoming wavelength in vacuum) hits the surface of the slab of thickness d, with an angle θ_i to the normal at the surface. This situation resembles figure 1. There are now two equations that must be solved together to calculate the conditions to have zero reflection. They are:

$$k_z = m\frac{\pi}{d} \tag{2}$$

which gives the the relation to have zero reflection in a uniform material. m is an integer number. Next, we must take into account the extra contribution to the wavevector parallel to the slab, k_x, coming from the periodicity:

$$k_x \to k_x + NG_x \tag{3}$$

where $G_x = 2\pi/a$ is the lattice constant in the reciprocal space and N is an integer number. Putting the two equations together and remembering that the wavevector parallel to the interface must be conserved, we obtain:

$$k_2^2 - (k_1 \sin\theta_i + NG_x)^2 = m^2\frac{\pi^2}{d^2} \tag{4}$$

where $k_i = k_0 n_i$, $i = 1, 2$, with k_0 being the wavevector in vacuum. Because for the zeroth diffracted order we have $N = 0$, we can simplify equation (4):

$$k_2^2 - k_1^2 \sin\theta_i^2 = m^2\frac{\pi^2}{d^2}. \tag{5}$$

In the case of the first diffracted order, $N = -1$, hence equation (4) becomes:

$$k_2^2 - (k_1 \sin\theta_i - G_x)^2 = m^2\frac{\pi^2}{d^2} \tag{6}$$

Let us now comment on the results. Equation (5) shows that, to maintain resonant conditions, when the angle θ_i increases then the thickness d must increase too. This is in agreement with the behavior of S_0 in figure 4(b). Vice versa, in equation (6), because of the inequality $G_x > k_1 \sin\theta_i$, we can easily see that the variables θ_i and d have an opposite relation than that in equation (5), namely θ_i increases when d decreases. This matches the behavior of the diffracted order S_1 in figure 4(b). However, in such a graph, the zeroth diffracted order also shows a dip moving to lower angles when the thickness d increases. Even though this seems to contradict equation (5), a simple consideration about energy conservation immediately suggests how it is the counterpart of the maximum in S_1. Furthermore, by looking at the shapes of both the zeroth and first diffracted orders, and considering the typical form of a Fano resonance, it seems safe to argue that they are associated with two different transmission paths [18]. In particular, the zeroth order recalls a Fabry–Perot mode (and the shift analysis supports such a statement), namely direct transmission through the slab, whereas the first order manifests the coupling of the incident light with quasi-guided modes of the slab. To conclude this paragraph, we have to notice that, to realize a precise prediction of the diffractive order behavior, instead of using the effective refractive index of the slab (valid only in the long wave approximation regime), we should consider the effective refractive index of the specific mode. Besides, equation (2) should take into account the reflection phase shift ϕ too, and so to become $k \to k + \phi/d$. These requests can be fulfilled easily by means of numerical simulations. However, the general conclusions just illustrated would maintain their validity.

3. Single-hole slab versus multi-hole slab

So far we have explained the transmission peaks through a photonic crystal slab as being due to the coupling between incoming light and quasi-guided modes. However, we could wonder if there exists any difference in transmission between a slab with a single hole and an infinite array of holes. To answer this question, a brief review of two-dimensional metallic sub-wavelength gratings is helpful. One of the often-considered channels for the enhancement of transmission in metallic sub-wavelength gratings is given by surface plasmon–polaritons. It is said that they play a key role in the enhancement process [1]. However, an alternative picture in which plasmon–polaritons are just one of the ingredients for realizing strong transmission has been introduced [5, 9]. In such a description, the enhancement is explained in terms of light interference in the metallic slab. Because the device analyzed here does not satisfy any of the conditions for manifesting metallic surface modes (for example, the dielectric function is never negative),

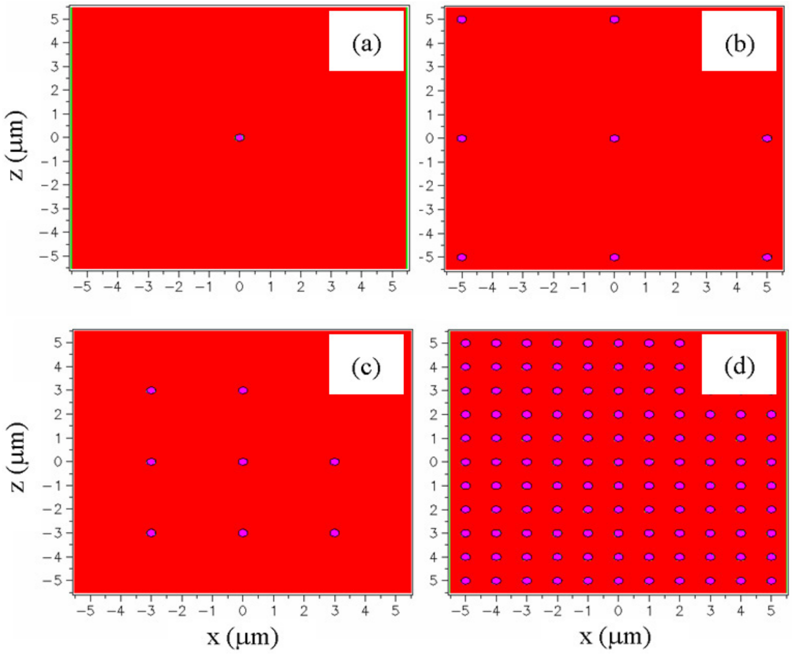

Figure 6. From (a) to (d), four situations are shown: single isolated hole ($a = \infty$), semi-isolated hole ($a = 5\ \mu$m), semi-communicating hole ($a = 3\ \mu$m) and communicating hole ($a = 1\ \mu$m), where a is the lattice constant. The holes are realized with SiO_2 and the slab with c-Si. The geometrical parameters are the same as in figure 3.

the interference method is definitely what we need to describe our results. In order to do this, a main consideration must follow. In [9], the interference pattern is calculated starting from the light diffracted by a single slit in an opaque screen. For such a reason, each hole of a thick metallic grating can be considered to be a point source, and an interference pattern can be calculated. Here, however, because of the choice of materials, the hypothesis of dealing with an opaque screen is no longer valid. Anyway, diffraction occurs in a dielectric photonic crystal too, hence we can assume that we have a pattern of point sources, respecting the symmetry of the slab, which can be described by means of the same approach used in [9]. The only difference from a metallic grating is that the point sources are not strictly defined inside the holes only. Hence a slightly different approach must be followed. In particular, we have to make a comparison between the power coming from a single unit cell (and not a hole only) of the periodic slab and an analogous domain (no longer a unit cell, because no periodicity is present) surrounded by uniform material. We first simulated an isolated single hole and next we introduced a periodicity a by means of some neighbours. Then we reduced the period of the crystal to fill the unit cell slowly to analyze the influence that single holes can have on each other. The geometrical and material parameters are the same as in figure 3, with $\lambda = 2.066a$. A schematic representation is shown in figure 6. In (a), an isolated hole is irradiated. Because the wavelength of the incident light is much bigger than the diameter of the hole, the transmission spectrum is expected to be similar to the case of a uniform slab. In (b), some neighbours are introduced into the slab. Their minimum distance from the central hole is five lattice constants. In (c), the condition of isolation of the central hole is further reduced by putting extra neighbours at just three lattice constants from the center. Finally, a periodic structure with periodicity equal to one is introduced (d). In all four cases, both the radius and the thickness of the slab are kept constant. As expected, from figure 7 we see that, moving from a single isolated hole (case (a)) to a periodic array of holes (cases (b) to (d)), Fano's peaks appear, showing that quasi-guided modes are realized inside the slab. Moreover, the closer the holes are, the stronger the Fano's peaks become. The mechanism for describing such a transmission enhancement is then consistent with the description which claims diffraction to be the only necessary frame for explaining extraordinary transmission, both in dielectric and in metal periodic structures. In figure 7(a), the graphs corresponding to a uniform slab (continuous line) and a single hole (dot line) are overlapped. This means that the light cannot feel the presence of a single hole, namely no diffraction occurs, at least for the geometrical parameters used in the simulations. The only channel available to light to cross the slab is through direct transmission. In the case of the absence of any holes, we find the typical etalon oscillations.

So far we have shown explicitly that the thickness of the slab, the angle of incidence and the wavelength are closely connected to giving the Fano resonance. However, nothing was really said about the role played by the radius of the holes. The reader could have correctly guessed that, in the calculation of the effective refractive index, the radius of the holes must be considered. Now we want to show another example where the only modification of the radius realizes a tuning of the resonant peaks. In figure 7(b), two curves are close to each other: one for the case at $r = 0.15a$ and the next for $r = 0.40a$. It is interesting to notice that, by increasing the radius, Fano peaks tend to become broader and to shift to lower wavelength. The reasons are the tendency of the light to be less localized inside

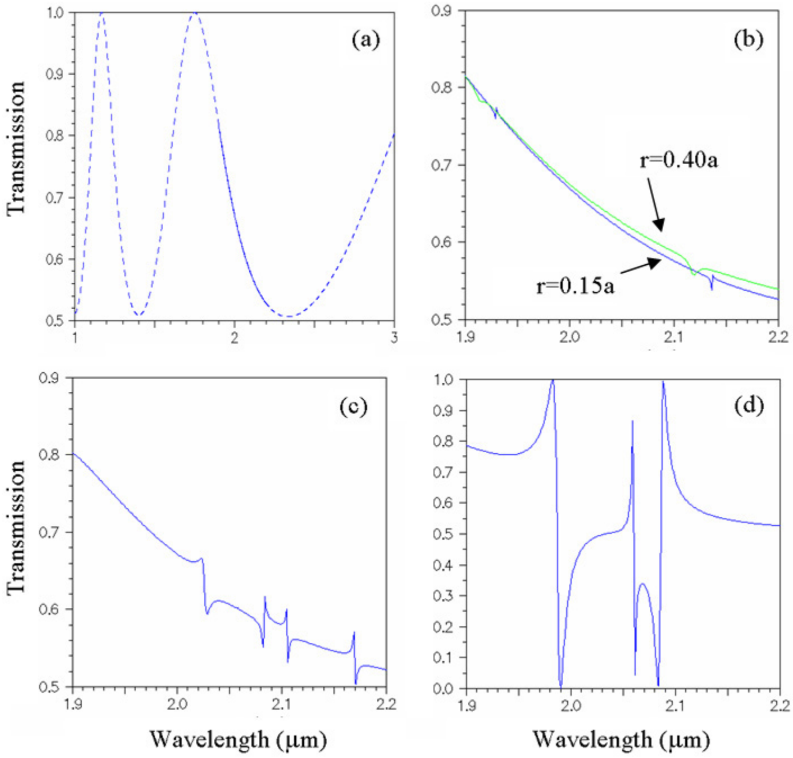

Figure 7. Total transmissions corresponding to the structures of figure 6 are shown. On increasing the density of the holes, the Fano peaks start to appear. When the holes are sufficiently close to each other, the Fano peaks are well defined (d). In (a), the overlap between a single hole (dot line) and a uniform slab (continuous line) are also realized. No differences occur. In (b), both the case at radius $r = 0.15a$ and the case at $r = 0.40a$ are shown. In the case of the bigger radius, the Fano peaks become broader and shift to shorter wavelengths. The thickness of the slab is $d = 0.5a$, the radius $r = 0.15a$, and $a = 1\ \mu$m is the lattice constant. The light is orthogonal to the plane of the slab.

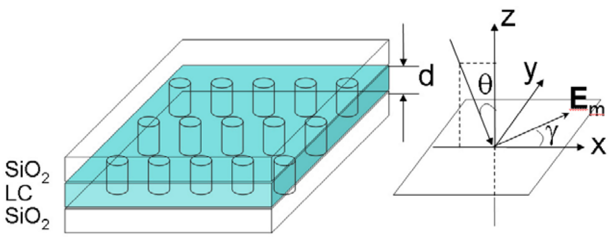

Figure 8. Liquid crystal (in dark) embedded in between SiO_2 layers. $\mathbf{E}_m$ is the manipulative field.

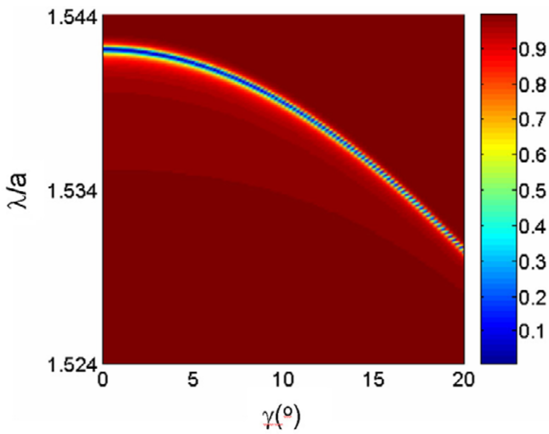

Figure 9. Transmission spectrum with external electric field $\mathbf{E}_m$ belonging to the x–y plane. The light polarization is along the x axis. γ is the angle between $\mathbf{E}_m$ and the x axis. λ is the wavelength of the incoming light. All the diffracted orders are considered here.

the slab as well as the reduction of the effective refractive index of the slab, respectively.

4. Liquid crystals in sub-wavelength dielectric slab

Liquid crystals (LC) are anisotropic substances which show both liquid and solid behavior, in the sense that, according to external conditions, they can either modify or maintain their own position. Some of the parameters that can be adjusted to control the orientation of liquid crystals are the temperature and the electric field. In particular, we are going to consider LC manipulation through an external electric bias. Because the refractive index depends on the crystal orientations, the natural conclusion is that the electric field can control the LC refractive index. The model investigated here is shown in figure 8. It consists of two-dimensional SiO_2 rods in a square pattern, grown on a SiO_2 substrate, surrounded by LC material. In the end, SiO_2 bulk is positioned to embrace the LC. The structure parameters are as follows: a is the lattice constant, the rod radius is $0.3a$ and the liquid crystal thickness is equal to $5a$. We assume an extraordinary refractive index $n_e = 1.706$ along the x axis and an ordinary refractive index $n_o = 1.522$ in both the y and z axes. From a practical point of view, such a design presents a drawback that is not easy to solve, namely the difficulty in maintaining the LC alignment. However, at this stage, we are interested in showing the strong

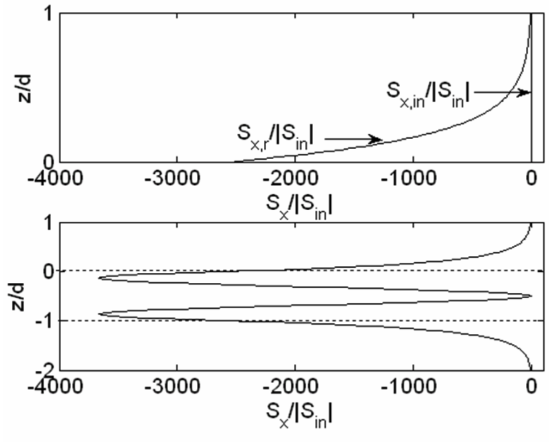

(a)

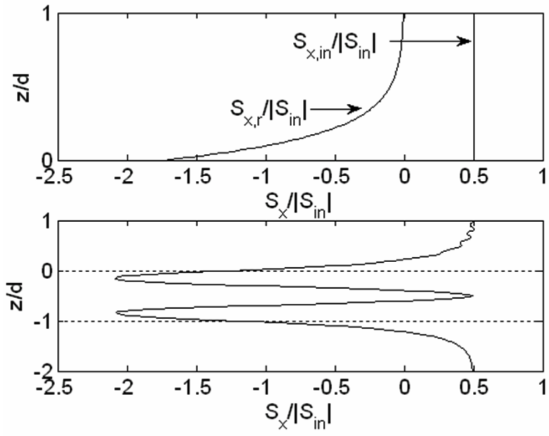

(b)

Figure 10. (a) and (b) illustrate the distribution of the component S_x of the Poynting vector of the photonic crystal slab. In (a) and (b) γ is equal to 0° and 5°, respectively. In other words, in (a) n_e is along x axis whereas in (b) it is along the direction forming 5° with x axis. The incoming light is at an angle $\theta = 30°$ from z (see figure 8) with polarization parallel to x axis and wavelength $\lambda = 2.2036a$. The Poynting vector is averaged on a unit cell. In (a) and (b) the top figures show the distribution of the incident component $S_{x,\text{in}}$ and reflection $S_{x,\text{r}}$ above the top layer of the slab; the bottom figures, illustrate the overall energy flux distribution across the slab (the last denoted by the the dot lines). d is the slab thickness. It is also important to notice that because of the scale in the abscissa, the top figure in (a) seems to show a value of $S_{x,\text{in}}/|S_{\text{in}}|$ equal to zero. However the real value is 0.5 (as expected considering that $\theta = 30°$). In these numerical simulations the totality of the diffracted orders were considered.

connection between the change in refractive index and the transmission shift, so that the deficiency mentioned is not an issue. If the incident light is along the z axis with polarization along the x direction and the electric field $\mathbf{E}_\text{m}$ shows an angle γ to the x axis, then the transmission spectrum illustrated in figure 9 is obtained. A Fano resonance is shown in the interval of wavelengths from $1.524a$ to $1.544a$. When the angle γ is increased, the peak moves to shorter wavelengths. In particular, changing the electric field orientation by 20° results in a Fano mode shift of 10 nm, at $a = 1\ \mu$m. Fano resonances occur when the energy is mainly confined inside the slab. This is because they represent the coupling between a continuum of states and discrete states. In particular, if the incident angle θ is 30° away from the z axis on the x–z plane, a Fano resonant wavelength of $2.2036a$ is obtained. Assuming such a value as the incoming wavelength, if the angle γ of the external electric field to the x axis is 0°, then the distribution of the Poynting vector component S_x is shown in figure 10(a). The abscissa represents the ratio between S_x and S_{in}, the last being the total energy flux of the incident light. We can see that the energy is concentrated inside the slab and it tends to flow along the negative x direction. Indeed, for the parameters corresponding to figure 10(a), both S_y and S_z are approximately zero. If the angle γ is changed to 5°, the energy flux inside the slab along the negative x direction is greatly reduced, as shown by figure 10(b). To understand such results better, we have also calculated the total transmission for both angles. In figure 11, the transmission at $\lambda = 2.2036a$ drops dramatically in the case of $\gamma = 0°$. Vice versa, for $\gamma = 5°$ the resonance is at $\lambda = 2.2043a$. Besides, confirmation of high energy storage inside the slab is given by the estimation of the quality factor Q, which is roughly 20 000.

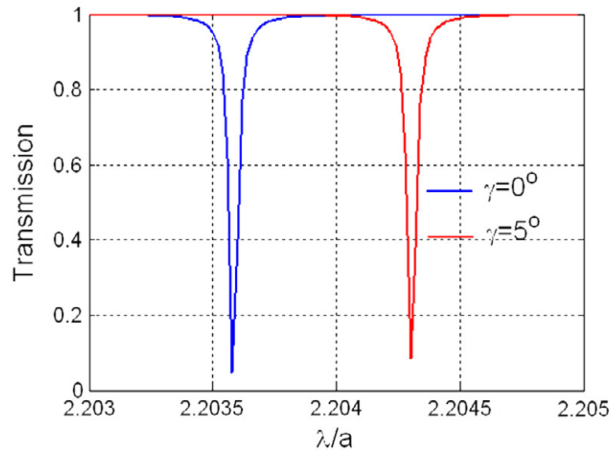

Figure 11. Total transmission for liquid crystal system when the electric field $\mathbf{E}_\text{m}$ is either at 0° or 5° from x axis. Two resonant peaks of high quality factor Q (about 20 000) occur at two different wavelengths.

Because of the obvious high sensitivity presented by the LC, such a structure can be utilized for a broad range of applications. For example, it can be used as a high-sensitivity electronic detector, or an optical coupler for waveguides. Another application is in the photoluminescence field. Indeed, filling organic dye into liquid crystals and irradiating the system with light at the Fano resonant wavelengths will result in an increase in the photoluminescence effect. In fact, at Fano resonances, as shown in figure 10, the energy is strongly confined *inside* the slab, being several thousands times bigger that the incident energy flux. Because of this, even compounds with a low quantum yield (the ratio between the numbers of emitted and absorbed photons) can realize efficient fluorescence.

5. Conclusion

In summary, we have investigated some of the physical phenomena that occur when light couples with a sub-wavelength photonic crystal slab. In particular, we have analyzed the influence of an array of holes on the transmission enhancement and described it in a diffraction frame. Moreover, we have shown that the manipulation of an external electric field acting on an anisotropic structure made of liquid crystals realizes tuning of the transmission peaks. Furthermore, high sensitivity dependence on the incident electric field orientation is also obtained. At Fano resonant wavelengths, photonic quasi-guided modes inside the liquid crystal layer are manifested. However, they are so sensitive to the electric field direction that its modification of only a few degrees makes the modes almost disappear. Such characteristics offer an initial hint for the realization of devices that are able to manipulate light, such as electric field detectors, switches, and so on.

References

[1] Ebbesen T W, Lezec H J, Ghaemi H F, Thio T and Wolff P A 1998 *Nature* **391** 667–9

[2] Porto J A, Garcia-Vidal F J and Pendry J B 1999 *Phys. Rev. Lett.* **83** 2845–8

[3] Popov E, Neviere M, Enoch S and Reinisch R 2000 *Phys. Rev.* B **62** 16100–8

[4] Martin-Moreno L, Garcia-Vidal F J, Lezec H J, Pellerin K M, Thio T, Pendry J B and Ebbesen T W 2001 *Phys. Rev. Lett.* **86** 1114–7

[5] Treacy M M J 2002 *Phys. Rev.* B **66** 195105

[6] Sarrazin M, Vigneron J P and Vigoureux J M 2003 *Phys. Rev.* B **67** 085415

[7] Barnes W L, Murray W A, Dintinger J, Devaux E and Ebbesen T W 2004 *Phys. Rev. Lett.* **92** 107401

[8] Koerkamp K J K, Enoch S, Segerink F B, van Hulst N F and Kuipers L 2004 *Phys. Rev. Lett.* **92** 183901

[9] Lezec H J and Thio T 2004 *Opt. Express* **12** 3629–51

[10] Miroshnichenko A E and Kivshar Y S 2005 *Phys. Rev.* E **72** 056611

[11] Gomez-Medina R, Laroche M and Saenz J J 2006 *Opt. Express* **14** 3730–7

[12] Moreno E, Martin-Moreno L and Garcia-Vidal F J 2006 *J. Opt. A: Pure Appl. Opt.* **8** S94–7

[13] Cao Q and Lalanne P 2002 *Phys. Rev.* B **66** 195105

[14] Ung B and Sheng Y 2007 *Opt. Express* **15** 1182

[15] Fano U 1961 *Phys. Rev.* **124** 1866–78

[16] Johnson S G, Fan S, Villeneuve P R, Joannopoulos J D and Kolodziejski L A 1999 *Phys. Rev.* B **60** 5751

[17] Song J F, Proietti Zaccaria R, Yu M B and Sun X W 2006 *Opt. Express* **14** 8812–26

[18] Fan S and Joannopoulos J D 2002 *Phys. Rev.* B **65** 235112

[19] Hessel A and Oliner A A 1965 *Appl. Opt.* **4** 1275–97